General Disclaimer

One or more of the Following Statements may affect this Document

- This document has been reproduced from the best copy furnished by the organizational source. It is being released in the interest of making available as much information as possible.

- This document may contain data, which exceeds the sheet parameters. It was furnished in this condition by the organizational source and is the best copy available.

- This document may contain tone-on-tone or color graphs, charts and/or pictures, which have been reproduced in black and white.

- This document is paginated as submitted by the original source.

- Portions of this document are not fully legible due to the historical nature of some of the material. However, it is the best reproduction available from the original submission.

Produced by the NASA Center for Aerospace Information (CASI)

VOLUME II

NASA CR-144917

APPLICATION TO A LARGE SPACE TELESCOPE

(NASA-CR-144917-Vol-2) ANNULAR MOMENTUM CONTROL DEVICE (AMCD). VOLUME 2: APPLICATION TO A LARGE SPACE TELESCOPE Final Report (Ball Bros. Research Corp.) 50 p HC $4.00 CSCL 13I G3/37

N76-19458

Unclas 20656

FINAL REPORT

ANNULAR MOMENTUM CONTROL DEVICE (AMCD)

PREPARED FOR

NATIONAL AERONAUTICS AND SPACE ADMINISTRATION
LANGLEY RESEARCH CENTER
HAMPTON, VIRGINIA

MAR 1976
RECEIVED
NASA STI FACILITY
INPUT BRANCH

Ball Brothers Research Corporation
SUBSIDIARY OF BALL CORPORATION

Aerospace Division
BOULDER, COLORADO 80302

F76-02

NASA CR-144917

FINAL REPORT

ANNULAR MOMENTUM CONTROL DEVICE (AMCD)

VOLUME II: APPLICATION TO A LARGE SPACE TELESCOPE

Prepared under Contract No. NAS 1-12529 by
Ball Brothers Research Corporation
Boulder, Colorado 80302

for

NATIONAL AERONAUTICS AND SPACE ADMINISTRATION

SUMMARY

The annular momentum control device (AMCD) is a thin hoop-like wheel with neither shaft nor spokes (see Frontispiece). The wheel floats in a magnetic field and can be rotated by a segmented motor. Potential advantages of such a wheel are low weight, configuration flexibility, a wheel that stiffens with increased speed, vibration isolation, and increased reliability.

The AMCD is nearly 2 meters (6 feet) in diameter. An annular aluminum baseplate supports the entire wheel assembly. Vacuum operation is possible by enclosing the wheel in an annular housing attached to the baseplate. The rotor or "rim" has a diameter of about 1.6 meters (63 inches) and consists principally of graphite-epoxy composite material. It weighs 22.5 kilograms (49.5 pounds) and is strong enough to be spun at 3000 rpm. At this speed, it can store 2200 N-m-s (3000 ft-lb-sec) of angular momentum. A system of pneumatic bearings can support the rim in the event of a magnetic suspension failure.

The magnetic suspension system supports the rim both axially and radially at three points. Combinations of permanent magnets and electromagnets at each of the three suspension stations exert forces on ferrite bands imbedded in the rotating rim. The magnetic gaps are about 0.25 cm (0.1 inch) above, below, and inside the rim. The gaps are maintained by servo loops with 50 hertz bandwidths that respond to error signals generated by inductive sensors. The servo loops can be operated in either "positioning" or "zero-power" modes.

The rim is accelerated and decelerated by a large diameter, segmented, brushless d.c. motor. Electromagnet stator segments are placed at each suspension station and interact with samarium cobalt permanent magnets placed every 7.3 cm (2.9 inches) along the periphery of the rim. Commutation is achieved by Hall sensors that detect the passing permanent magnets.

Volume I of this report describes the analysis, design, fabrication, and testing of the laboratory model of the AMCD. Volume II contains a conceptual design and set of dynamic equations of a gimbaled AMCD adapted to a Large Space Telescope (LST). Such a system could provide maneuver capability and precision pointing by means of one external gimbal, wheel speed control, and small motions of the rim within the magnetic gap.

TABLE OF CONTENTS

1.0 APPLICATION

The application of an AMCD to a Large Space Telescope (LST) is just one of many possible ways in which an AMCD can be used. This application makes use of the fine pointing capability of the AMCD, which is extremely important for a system such as LST, but it does introduce some problems as well. The LST mission will require pointing the entire spacecraft at many different astronomical targets, limited only by stray light effects when pointed too close to the sun line. As a result, the LST will maneuver through larger angles many times. Since the momentum stored in the AMCD is large and since much control effort would be needed to move this momentum vector in space, the AMCD must be in a gimbal. Another problem is that a fairly wide magnetic gap must be provided so that external disturbance torques can be accumulated for long periods of time without moving the coarse gimbal system. Motions of the coarse gimbal will upset the fine pointing.

In this short study, a preliminary design was developed for the deployment mechanisms, gimbal, and wheel. Equations of motion were also developed.

2.0 SYSTEM DESCRIPTION

The AMCD would be attached to the LST as shown in Figure 2-1. A single gimbal is used and it is arranged so that when the H vector is aligned with the sun line, the extendable light shield on the front of the telescope is always on the sunny side of the telescope. All points in the celestial sphere (except those within 45 degrees of the sun) can be seen by rolling about the sun line (speeding up or slowing down the wheel) and gimbaling the wheel through a range of 135 degrees. Alignment of the H

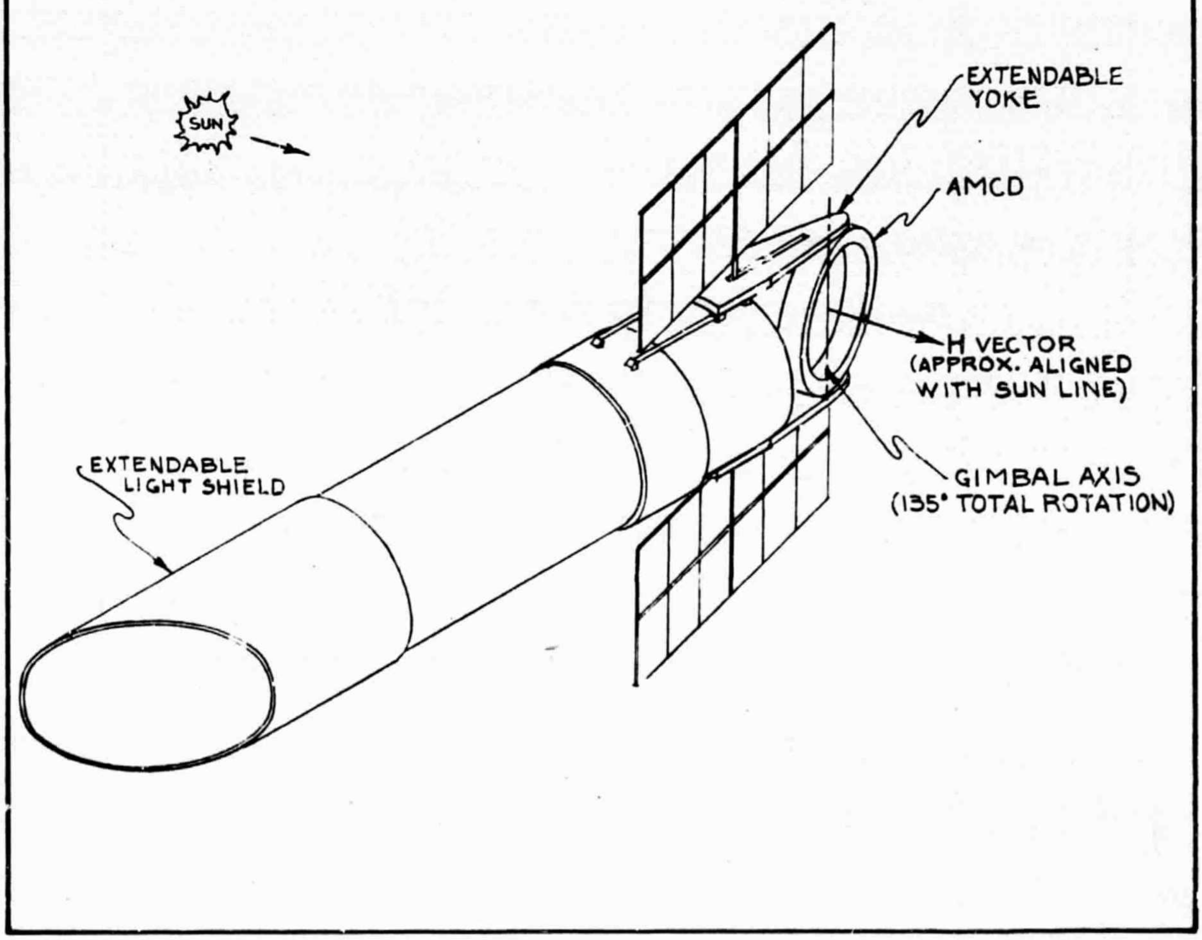

Figure 2-1 AMCD on a Large Space Telescope

vector with the sun line need not be perfect. If, however, the misalignment of the H vector with the sun line becomes large enough because of external torques to give light shield alignment problems, reaction jets on the LST can be used to reposition the H vector. This pointing scheme in which a single gimbal aligns the H vector with the sun line was conceived at Langley Research Center.

Fine pointing is achieved by using the inherent features of the AMCD. By means of gimbaling the rim within the magnetic gap and by means of speed control of the wheel, full three-axis fine pointing can be achieved. The three control axes are not necessarily aligned with the sensor axes of the LST but a simple coordinate transformation based on the gimbal angle can convert LST errors into the AMCD coordinate frame. It should be noted that "gimbal lock" conditions cannot occur. The three control axes are fixed to the gimbal ring and are always orthogonal no matter what the gimbal angle is. Further, it should be noted that the gimbal is used only for coarse maneuvers from one target to another. Motion of this gimbal during fine pointing would not be tolerable.

Launching of the LST with the AMCD as shown in Figure 2-1 would be awkward. Thus, a deployment mechanism is required. In the system shown, the wheel is stowed flat against the back end of the LST during launch. The extendable yoke moves it to its deployed position once in orbit. The LST concept has included a refurbishment plan in which astronauts would change and repair instruments in the back end of the telescope. This access could be provided in spite of the AMCD system being on the back end. When access to the instruments is required, the AMCD would be retracted and the astronauts could enter the telescope through the center of the AMCD.

3.0 DESIGN CONDISERATIONS

A conceptual mechanical arrangement of the LST system is shown in Figure 3-1. Design of the gimbal system and extension arms is based on the requirement that they will not require extensive modification of the present LST structures. The orientation of the gimbal axis parallel to the solar array struts and the small cross section available for extension arm structure combine to obviate an optimum lightweight design. The extension arms are made of aluminum honeycomb core 20 cm (8 inches) thick faced with .64 cm (.25 inches thick) aluminum plate and is curved to conform to the outer diameter of the LST. Resonant frequency is >11 hz and the arms have a mass of about 225 Kg each.

The arms are mounted on rails fixed to the LST. The rails guide the arms during deployment and retraction of the gimbal system. Latches fix the arms to the LST in the launch and deployed positions. The latches isolate the deployment drive system from launch and maneuver loads imposed by the extension arms and gimbal. This permits the use of a reasonably lightweight chain and sprocket driven by servo-controlled torque motors. The servo control will maintain the extension arm geometry during deployment and retraction. When deployed, the center of the AMCD is 6.88 m(271 in.) from the OTA-SSM interface on the LST.

The gimbal actuator consists of synchronized torque motors mounted on each side of the gimbal ring. The torque motors are 15 N-m (11 ft-lb) units as used for fine pointing on the Apollo Telescope Mount. A resolver senses angular position in one actuator. Gimbal bearings are back-to-back mounted angular contact ball bearings. The bearings are retained in temperature compensating stainless steel sleeves in the aluminum actuator housing. Motor and bearing lubrication is provided by a BBRC Vac Kote system incorporating lubricant reservoirs and labyrinths to control outgassing. Flex cables operate through a 180° angle of rotation

ORIGINAL PAGE IS
OF POOR QUALITY

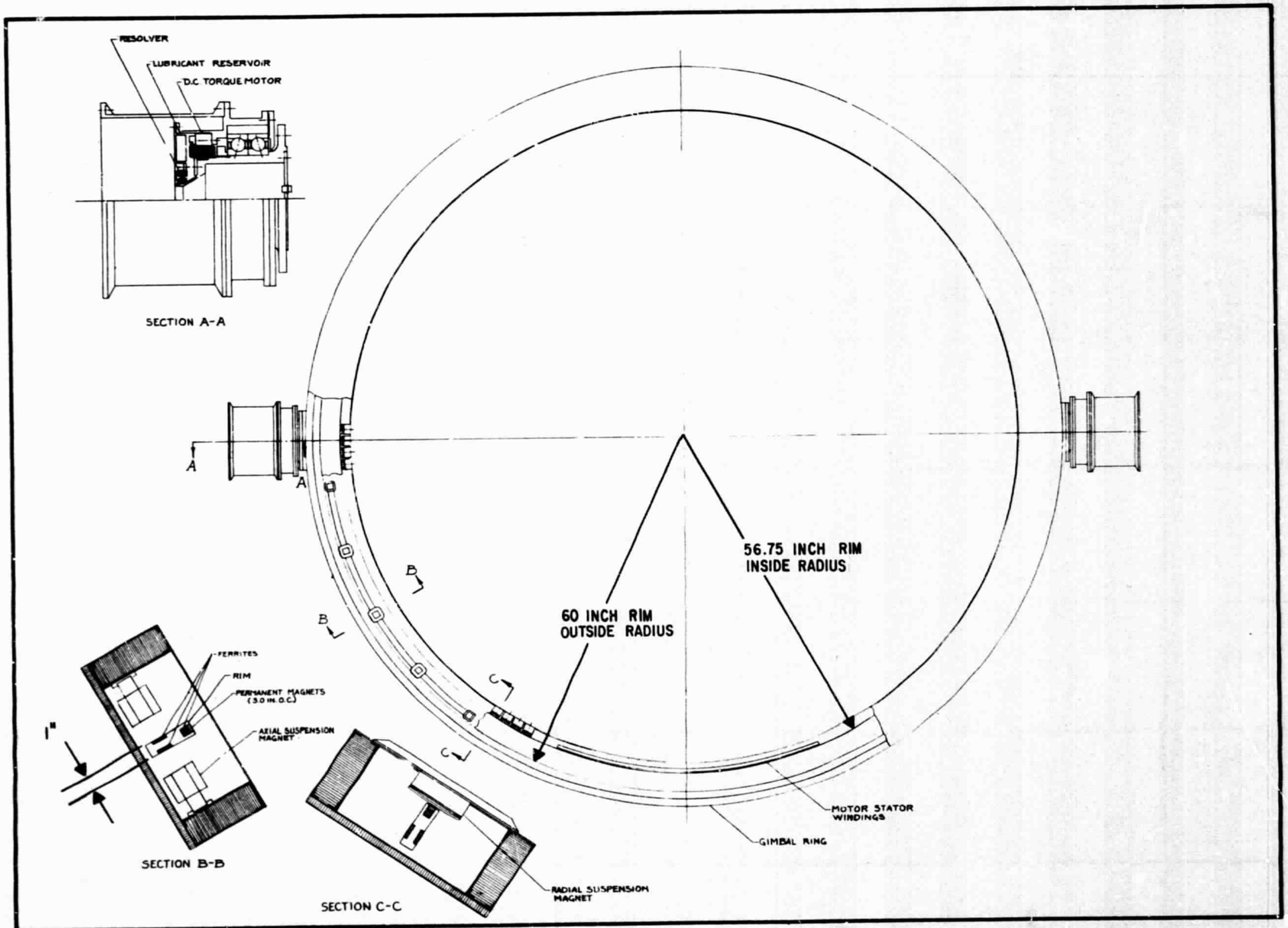

Figure 3-1 AMCD For The LST

F76-02

to transmit power and signals across the gimbal interface. The actuator module permits ease of assembly to the extension arm and gimbal structure.

The LST AMCD rim weighs 44 Kg and provides 16,000 N-m-sec (12,000 ft-lb-sec) of angular momentum at a spin rate of about 1500 rpm. The rim outside diameter is twice that of the laboratory AMCD rim and it has a spin moment of inertia of 93 Kg-m^2. At design speed the stress levels are the same as for the original rim. The graphite/epoxy composite structure of the rim has continuous channels on the top, bottom and inner surfaces of the rim which retain the ferrites for the magnetic suspension and samarium cobalt magnets for the motor.

The motor magnets are relocated to the inner surface in order to keep a more constant magnetic gap as the rim moves up and down. The stator coils lie on one side of the magnets rather than on both sides as in the laboratory AMCD. The stator coils must be very wide so that active conductors are always opposite the magnets even though the rim moves ±3.8 cm (±1.5 inches). The return path for magnet flux is through the ferrite band behind the magnets. Commutation of the motor would be by means of Hall sensors as in the laboratory AMCD.

The radial suspension system is the same as used in the laboratory AMCD except that the support magnets must be rotated as shown. This allows the rim to have large axial motions and yet not move out of the range of the support magnets. Of course, the radial forces that can be generated will be lower but radial disturbances are very small too. Some increase in drag will occur because of the radial ferrite band undergoing a change in flux as it passes under each magnet.

The axial suspension system is considerably different from that of the laboratory AMCD and the reason is the enormous magnetic

gap that must be accommodated. Fortunately only about 13 newtons need to be generated in the LST case as opposed to about 180 newtons in the laboratory device.

The first consideration is pole separation. The poles of the support magnets must be far enough apart to induce the flux to pass through the rim rather than just jump the gap from pole to pole. In order to keep the same relationship between pole separation and gap as was used in the laboratory model, a pole separation of at least 30 cm (12 inches) is required. Since the rim is not 30 cm wide, the poles must be placed circumferentially. The flux then passes through the ferrite bands circumferentially rather than radially.

Pole "saliency" is important, too, or leakage flux will be extremely high. Saliency is the amount the poles protrude beyond the common circumferential "core" of the magnets. A saliency of 5 cm (2 inches) is used because this is larger than the gap. Tests would have to be performed to determine if this is sufficient.

Sensing the rim displacement is not simple, the capacitive and "eddy current" systems used on the laboratory AMCD may not be able to cope with the large axial motions. We have assumed that rim motion is sensed by an electro-optical nulling system at each station. A high contrast stripe on the rim surface is illuminated and the stripe image is focused on a two element photodiode. Displacement of the rim results in a differential output signal from the photo-diodes. Variations of this system were used with considerable success on the ATM/SKYLAB HAO coronagraph internal alignment system.

The gimbal ring structure is fabricated of honeycomb sandwich material. The upper and lower suspension units are mounted to 5 cm (2 inches) thick honeycomb rings. The outer surface of the rings are fastened to a 1.27 cm (.50 inch) thick honeycomb shell with machined transition housings 180° apart to mount the gimbal actuator modules. The inner surface of the gimbal ring is .23 cm (.090 inch) aluminum with stiffened panels that mount the radial suspension magnets. The motor stators are less critical to align and are mounted to the .23 cm structure. This method of construction permits critical alignment of the suspended magnets on each ring before integration of the gimbal system. The thick honeycomb section of the rings is intended to maintain the necessary flatness of the magnet pole face plane when integrated with the other gimbal structures. The deep section gimbal ring is intended to provide a rigid stable structure for the AMCD. The gimbal ring has a mass of 245 Kg. This gives it moments of inertia of 488, 280, and 206 Kg-m^2 about the X, Y, and Z axes.

A retention system cages the rim during launch and when the AMCD is retracted to permit docking of the LST with shuttle. The jawed retainers will be deployed and retracted by stepper motors. The jaws will be surfaced with polyurethane elastomer to protect the rim surface. Actuation of the retainers would take place with the rim magnetically suspended but not rotating.

4.0 Equations of Motion

A large space telescope can achieve fine pointing through large angles using the configuration shown in Figure 4-1.

Coarse pointing is obtained analagous to an earth based telescope by first rolling about the "azimuth" axis then gimballing about the "elevation" axis. Roll is obtained by varying the

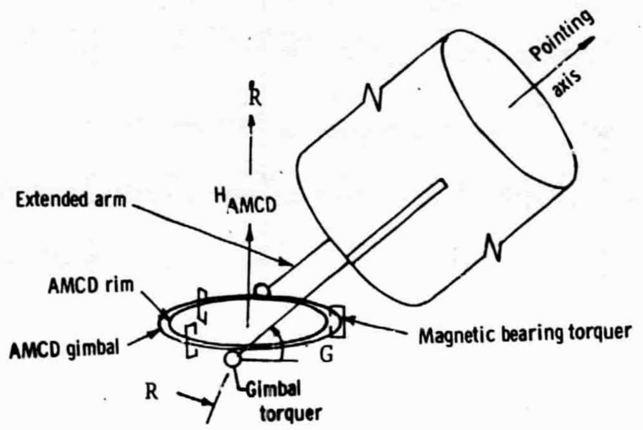

Figure 4-1 Single Gimbal AMCD-LST Configuration

speed control on the AMCD. Gimballing is accomplished by torquing the LST against the AMCD momentum. Fine pointing is obtained by locking the gimbal and tilting the gimbal ring in the air gap by again torquing against the AMCD momentum.

During maneuvers, the LST and AMCD both rotate about the system center of mass as shown in Figure 4-2. The resulting translational acceleration of the rim is caused by the gimbal ring-to-rim control forces which hold the rim in the air gap. To perform a pure roll maneuver as shown in Figure 4-2(A), the AMCD spin axis servo must change the spin rate of the rim to cause a gimbal ring roll rate. Concomitantly, the AMCD radial servos must go to work to keep the rim in the air gap because of the resulting translational acceleration. Similarly, to perform a

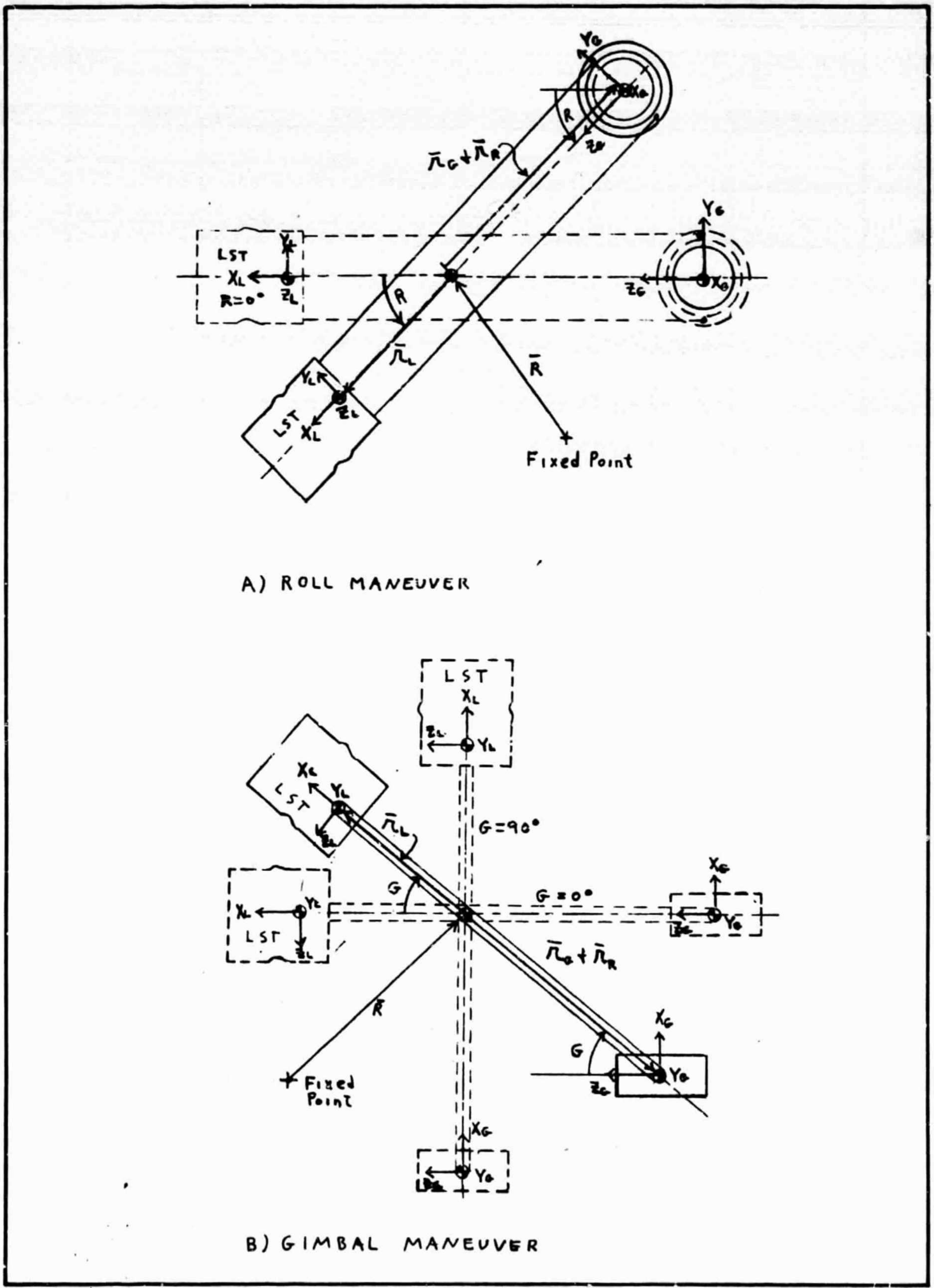

Figure 4-2 AMCD-LST Maneuvers

ORIGINAL PAGE IS
OF POOR QUALITY

pure gimbal maneuver as shown in Figure 4-2(B), the gimbal torques the LST by reacting against the AMCD momentum. This causes the AMCD axial servos to go to work to both restore the tilt of the gimbal ring with respect to the rim and to keep the rim positioned in the air gap while it is accelerating in translation.

To analyze the complicated coupling which exists among the servos during maneuvers, the equations of motion of the system need be developed. That is the purpose of this section.

4.1 List of Symbols

Abbreviations

AA: Angular Acceleration
AM: Angular Momentum
AMCD: Annular Momentum Control Device
AV: Angular Velocity
CG, SG: Cos G, Sin G
CP, SP: Cos P, Sin P
CR, SR: Cos R, Sin R
CY, SY: Cos Y, Sin Y
LST: Large Space Telescope
MI: Moment of Inertia
Wrt: With respect to

Angular Momentum

H_{AMCD}: component of rim AM along rim spin axis
$\bar{H}_G$, $\dot{\bar{H}}_G$: gimbal AM and its derivative
$\bar{H}_L$, $\dot{\bar{H}}_L$: LST AM and its derivative
$\bar{H}_R$, $\dot{\bar{H}}_R$: rim AM and its derivative

Angular Velocities and Accelerations:

- $\bar{\Omega}_G$: Inertial AV of gimbal
- $\bar{\Omega}_L$: Inertial AV of LST
- $\bar{\Omega}_R$: Inertial AV of rim
- P_G, Q_G, R_G: Components of $\bar{\Omega}_G$ along X_G, Y_G, Z_G respectively
- $\dot{P}_G$, $\dot{Q}_G$, $\dot{R}_G$: Their time derivatives
- P_L, Q_L, R_L: Components of $\bar{\Omega}_L$ along X_L, Y_L, Z_L respectively
- $\dot{P}_L$, $\dot{Q}_L$, $\dot{R}_L$: Their time derivatives
- P_R, Q_R, R_R: Components of $\bar{\Omega}_R$ along X_R, Y_R, Z_R respectively
- $\dot{P}_R$, $\dot{Q}_R$, $\dot{R}_R$: Their time derivatives
- P_S: Spin rate of rim relative to frame $X_R Y_R Z_R$
- $\dot{P}_S$: its time derivative

Centers of Mass

- CM: System center of mass
- CM_G: gimbal ring center of mass
- CM_L: LST center of mass
- CM_R: AMCD rim center of mass

Coordinate Frame

- $X_G Y_G Z_G$: frame fixed to gimbal ring with X_G normal to gimbal plane
- $X_I Y_I Z_I$: Inertial Frame
- $X_L Y_L Z_L$: Frame fixed to the LST with X_L out the pointing axis and Z_L toward the sun side.
- $X_R Y_R Z_R$: Nonspinning frame fixed to rim spin axis such that X_R lies along the spin axis

Euler Angles and Rates

β: gimbal euler angle = 270° + G

P
R
Y
Euler angles which orient $X_GY_GZ_G$ wrt $X_IY_IZ_I$
The order is Y (Yaw) about Z_I followed by P (Pitch) about the intermediate Y-axis followed by R (Roll) about X_G

$\dot{P},\dot{R},\dot{Y}$: Their time derivatives

G: Euler angle which orient $X_LY_LZ_L$ wrt $X_GY_GZ_G$ by rotating about Y_G.

$\dot{G}$: its time derivative

G_c: servo gimbal command

R_c: servo roll command

ψ,θ: Euler angles which orient $X_RY_RZ_R$ wrt $X_GY_GZ_G$ in order ψ about Z_G followed by θ about Y_R.

$\dot{\psi},\dot{\theta}$: Their time derivatives

ψ_c,θ_c: servo rim commands

Forces

F_{GLX}, F_{GLY}, F_{GLZ}: Interbody forces imparted by gimbal ring on LST at hinge line in directions parallel to X_G, Y_G, Z_G respectively

F_{GRX}, F_{GRY}, F_{GRZ}: Interbody forces imparted by gimbal ring on the rim acting at CM_R parallel to X_R, Y_R, Z_R respectively

F_{GX}, F_{GY}, F_{GZ}: Interbody forces imparted by LST and rim on gimbal acting at CM_G parallel to X_G, Y_G, Z_G respectively

F_{LX}, F_{LY}, F_{LZ}: F_{GLX}, G_{GLY}, F_{GLZ} resolved into directions parallel to X_L, Y_L, Z_L respectively.

Masses

M_G: gimbal ring mass

M_L: LST mass

M_R: rim mass

Moments of Inertia

I_{GX}, I_{GY}, I_{GZ}: MI of gimbal ring about X_G, Y_G, Z_G respectively
I_{LX}, I_{LY}, I_{LZ}: MI of LST about X_L, Y_L, Z_L, respectively
I_S: rim spin axis MI
I_T: rim transverse axis MI

Position Vectors and Distances

d_L: distance CM to CM_L
ℓ: distance gimbal hinge line to CM_L
$\bar{R}$: vector from inertially fixed point to CM
$\bar{r}_G$: vector from CM to CM_G
$\bar{r}_R$: vector from CM_G to CM_R
$\bar{r}_L$: vector from CM to $CM_L = \bar{i}_L d_L$

Torques

T_{GLX}, T_{GLY}, T_{GLZ}: Interbody torques imparted by gimbal ring on LST at hinge line in directions parallel to X_G, Y_G, Z_G respectively
T_{GRX}, T_{GRY}, T_{GRZ}: Interbody torques imparted by gimbal ring on the rim acting parallel to X_R, Y_R, Z_R respectively
T_{GX}, T_{GY}, T_{GZ}: Interbody torques imparted by LST and rim on gimbal acting parallel to X_G, Y_G, Z_G respectively
T_{LX}, T_{LY}, T_{LZ}: T_{GLX}, T_{GLY}, T_{GLZ} resolved into directions parallel to X_L, Y_L, Z_L respectively

Translations and Translational Accelerations

$\ddot{X}_G$, $\ddot{Y}_G$, $\ddot{Z}_G$: Inertial translational acceleration of gimbal ring parallel to X_G, Y_G, Z_G respectively
$\ddot{X}_{GR}$, $\ddot{Y}_{GR}$, $\ddot{Z}_{GR}$: relative translational acceleration between rim and gimbal

$\ddot{X}_{GRI}$, $\ddot{Y}_{GRI}$, $\ddot{Z}_{GRI}$: $\ddot{X}_{GR}$, $\ddot{Y}_{GR}$, $\ddot{Z}_{GR}$ resolved into inertial axes

$\ddot{X}_L$, $\ddot{Y}_L$, $\ddot{Z}_L$: Inertial translational acceleration of LST parallel to X_L, Y_L, Z_L respectively

$\ddot{X}_R$, $\ddot{Y}_R$, $\ddot{Z}_R$: Inertial translational acceleration of rim parallel to X_R, Y_R, Z_R respectively

x_{GRI}, y_{GRI}, z_{GRI}: rim displacement wrt gimbal expressed in inertial frame.

x_{GR}, y_{GR}, z_{GR}: x_{GRI}, y_{GRI}, z_{GRI} resolved paralled to X_G, Y_G, Z_G respectively

4.2 Summary of Equations

The system contains three separate parts: the LST, the gimbal ring, and the rim. Each part has three rotational and three translational degrees of freedom yielding a total of nine rotational and nine translational degrees of freedom. Because the system is physically held together or constrained, not all the degrees of freedom are independent. For example, the LST rotates and translates just like the gimbal ring except for the one degree of freedom between them, the gimbal angle. Consequently the two body system composed of the LST and gimbal ring have only four independent rotational degrees of freedom and three independent translational degrees of freedom, or a total of only seven independent degrees of freedom. The variables corresponding to these seven independent degrees of freedom are solved for from the dynamical equations. The variables of the five remaining dependent degrees of freedom are solved for by constraint equations which are kinematical equations expressing these variables in terms of the independent variables. The system then has seven independent rotational and two dependent rotational degrees of freedom and six independent translational and three dependent translational degrees of freedom.

The gimbal ring is oriented with respect to inertial space by three rotations. The LST is oriented with respect to the gimbal ring by one rotation. The spin axis of the rim is oriented with respect to the gimbal ring by two rotations. The Euler angle rates corresponding to the above rotations or Euler angles are functions of the independent body rates. The Euler angles are obtained by integrating the rates.

The complete set of equations of motion, containing no algebraic loops, are listed below where by convention $\sin(X) \triangleq SX$ and $\cos(X) \triangleq CX$. The right-hand equation numbers refer to the sequential equation numbering used in Section 4.3, Derivation of Equations.

Independent Degrees of Freedom:

1. $\dot{P}_G = I_{GX}^{-1}[T_{GX}+(I_{GY}-I_{GZ})Q_G R_G]$ (4-28)
2. $\dot{Q}_G = I_{GY}^{-1}[T_{GY}+(I_{GZ}-I_{GX})R_G P_G]$ (4-28)
3. $\dot{R}_G = I_{GZ}^{-1}[T_{GZ}+(I_{GX}-I_{GY})P_G Q_G]$ (4-28)
4. $\dot{P}_R+\dot{P}_S = I_S^{-1}T_{GRX}$ (4-16)
5. $\dot{Q}_R = I_T^{-1}[T_{GRY}+(I_T-I_S)R_R P_R-I_S R_R P_S]$ (4-16)
6. $\dot{R}_R = I_T^{-1}[T_{GRZ}+(I_S-I_T)P_R Q_R+I_S P_S Q_R]$ (4-16)
7. $\dot{Q}_L = I_{LY}^{-1}[T_{LY}+\ell F_{LZ}+(I_{LZ}-I_{LX})R_L P_L]$ (4-22)
8. $\ddot{X}_R = M_R^{-1}F_{GRX}$ (4-13)
9. $\ddot{Y}_R = M_R^{-1}F_{GRY}$ (4-13)
10. $\ddot{Z}_R = M_R^{-1}F_{GRZ}$ (4-13)
11. $\ddot{X}_G = M_G^{-1}F_{GX}$ (4-25)
12. $\ddot{Y}_G = M_G^{-1}F_{GY}$ (4-25)
13. $\ddot{Z}_G = M_G^{-1}F_{GZ}$ (4-25)

Constraint Degrees of Freedom:

14. $\dot{P}_L = SG\dot{P}_G + CG\dot{R}_G$ (4-23)

15. $P_L = SGP_G + CGR_G$ (4-23)

16. $\dot{R}_L = -CG\dot{P}_G + SG\dot{R}_G$ (4-23)

17. $R_L = -CGP_G + SGR_G$ (4-23)

18. $P_R = P_G + \Psi Q_G - \theta R_G - \theta\dot{\Psi}$ (4-8)

19. $P_S = (P_R + P_S) - P_R$ (4-46)

20. $\ddot{X}_L = -(R_L^2 + Q_L^2)d_L$ (4-33)

21. $\ddot{Y}_L = (\dot{R}_L + P_L Q_L)d_L$ (4-33)

22. $\ddot{Z}_L = (-\dot{Q}_L + P_L R_L)d_L$ (4-33)

Two unnecessary integrations are saved by resolving body rates as well as acceleration from independent variables, rather than obtaining the rates by integrating the resolved accelerations.

Euler Angle Rates:

23. $\dot{Y} = (Q_G SR + R_G CR)/CP$ (4-3)

24. $\dot{P} = Q_G CR - R_G SR$ (4-4)

25. $\dot{R} = P_G + SP\dot{Y} = P_G + \tan P(Q_G SR + R_G CR)$ (4-5)

26. $\dot{\Psi} = R_R - \theta P_R - R_G$ (4-9)

27. $\dot{\theta} = Q_R + \Psi P_G - Q_G$ (4-9)

28. $\dot{G} = Q_L - Q_G$ (4-12)

Constrained Forces and Torques:

29. $F_{LX} = M_L\ddot{X}_L$ (4-19)

30. $F_{LY} = M_L\ddot{Y}_L$ (4-19)

31. $F_{LZ} = M_L\ddot{Z}_L$ (4-19)

32. $F_{GLX} = SGF_{LX}-CGF_{LZ}$ (4-17)

33. $F_{GLY} = F_{LY}$ Inverted (4-17)

34. $F_{GLZ} = CGF_{LX}+SGF_{LZ}$ (4-17)

35. $T_{LX} = I_{LX}\dot{P}_L-(I_{LY}-I_{LZ})Q_LR_L$ (4-22)

36. $T_{LZ} = I_{LZ}\dot{R}_L-(I_{LX}-I_{LY})P_LQ_L+\ell F_{LY}$ (4-22)

37. $T_{GLX} = SGT_{LX}-CGT_{LZ}$ (4-18)

38. $T_{LY} = T_{GLY}$ Inverted (4-18)

39. $T_{GLZ} = CGT_{LX}+SGT_{LZ}$ (4-18)

Gimbal to Rim Displacement:

40. $\ddot{X}_{GR} = \ddot{X}_R-\ddot{X}_G$ (4-38)

41. $\ddot{Y}_{GR} = \ddot{Y}_R-\ddot{Y}_G$ (4-38)

42. $\ddot{Z}_{GR} = \ddot{Z}_R-\ddot{Z}_G$ (4-38)

43. $\ddot{X}_{GRI} = CPCY\ddot{X}_{GR}+(SRSPCY-CRSY)\ddot{Y}_{GR}+(CRSPCY+SRSY)\ddot{Z}_{GR}$ (4-42)

44. $\ddot{Y}_{GRI} = CPSY\ddot{X}_{GR}+(SRSPSY+CRCY)\ddot{Y}_{GR}+(CRSPSY-SRCY)\ddot{Z}_{GR}$ (4-42)

45. $\ddot{Z}_{GRI} = -SP\ddot{X}_{GR}+SRCP\ddot{Y}_{GR}+CRCP\ddot{Z}_{GR}$ (4-42)

46. $X_{GRI} = \iint\ddot{X}_{GRI}dtdt$ (4-43)

47. $y_{GRI} = \iint \ddot{Y}_{GRI} dtdt$ (4-43)

48. $z_{GRI} = \iint \ddot{Z}_{GRI} dtdt$ (4-43)

49. $x_{GR} = CPCYx_{GRI} + CPSYy_{GRI} - SPz_{GRI}$ (4-44)

50. $y_{GR} = (SRSPCY - CRSY)x_{GRI} + (SRSPSY + CRCY)y_{GRI} + SRCPz_{GRI}$ (4-44)

51. $z_{GR} = (CRSPCY + SRSY)x_{GRI} + (CRSPSY - SRCY)y_{GRI} + CRCPz_{GRI}$ (4-44)

Control Forces and Torques:

52. $F_{GRX} = f(x_{GR}, \theta, \Psi, \theta c, \Psi c)$ (4-36)

53. $F_{GRY} = f(y_{GR})$ (4-36)

54. $F_{GRZ} = f(z_{GR})$ (4-36)

55. $T_{GRX} = f(Ps, R, Rc)$ (4-37)

56. $T_{GRY} = f(F_{GRX})$ (4-37)

57. $T_{GRZ} = f(F_{GRX})$ (4-37)

58. $T_{GLY} = f(G, Gc)$ (4-35)

where $\theta c, \Psi c$, Rc, and Gc are control commands.

Gimbal Forces and Torques:

59. $F_{GX} = -F_{GRX} - F_{GLX}$ (4-24)

60. $F_{GY} = -F_{GRY} - F_{GLY}$ (4-24)

61. $F_{GZ} = -F_{GRZ} - F_{GLZ}$ (4-24)

62. $T_{GX} = -T_{GRX} - T_{GLX}$ (4-24)

63. $T_{GY} = -T_{GRY} - T_{GLY}$ (4-24)

64. $T_{GZ} = -T_{GRZ} - T_{GLZ}$ (4-24)

This completes the set and forms 64 equations in 64 unknowns. The equations are sorted and arranged in a logical flow diagram for programming their solution in Figure 4-3. The rotational equations are shown in Figure 4-3(A) and the translational equations in Figure 4-3(B).

4.3 Derivation of Equations

Assumptions

The equations of motion are derived subject to the following assumptions:

- The rim translates and rotates with respect to the gimbal through very small distances and angles.
- This implies that the rim planar forces cause the rim to translate radially without tending either to tilt the rim or to translate it axially. It further implies that the forces normal to the rim plane causes the rim to translate axially and to rotate without tending to cause it to translate radially.
- The small rim-gimbal relative translation and rotation assumption also implies that the centers of mass of the LST, total system, gimbal ring, and rim may be considered to lie along a straight line. This assumption allows the torques due to interbody forces which are collinear with the attaching arm to be ignored. Further, the centers of mass of the gimbal ring and rim are assumed always coincident.

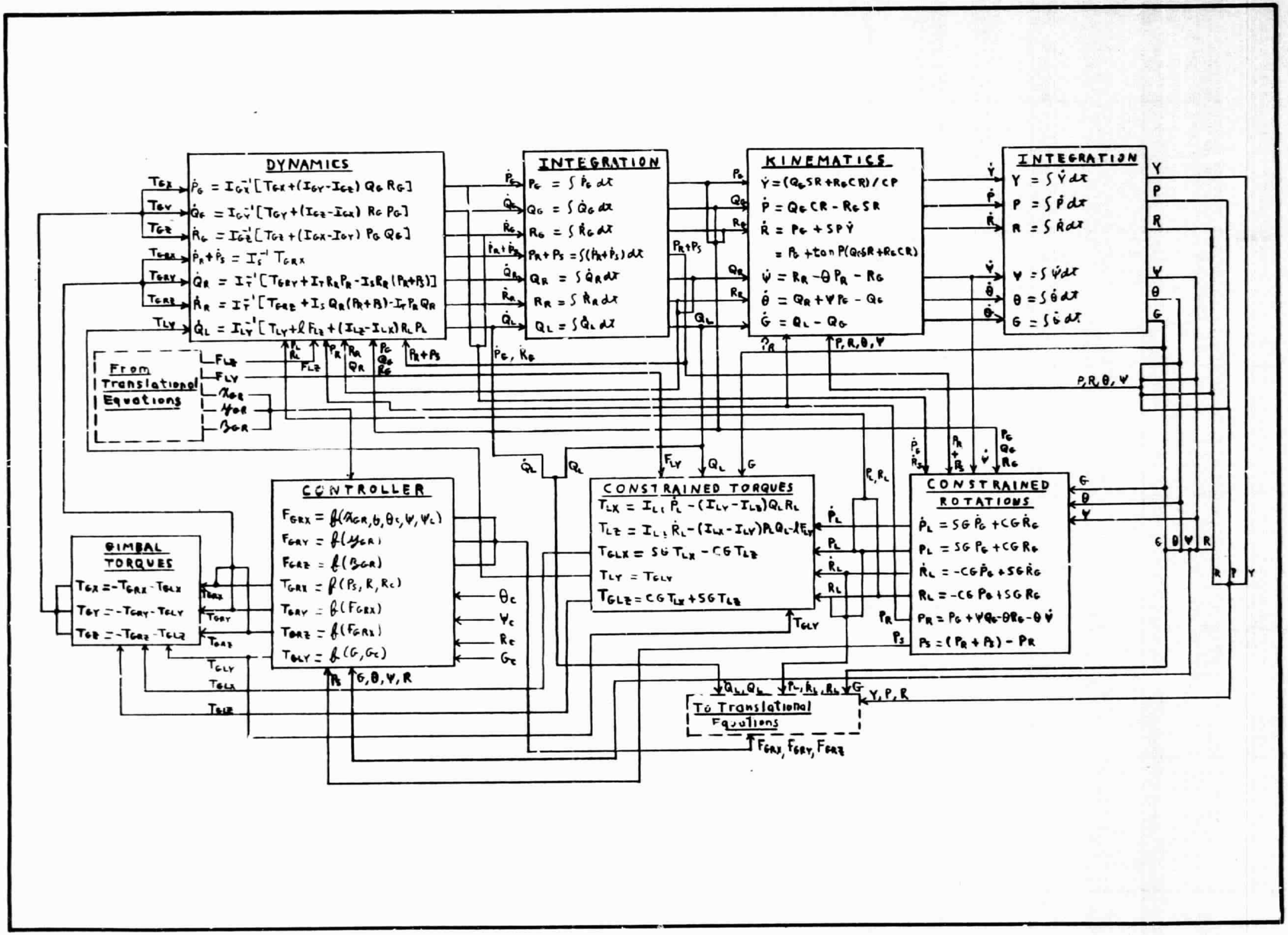

Figure 4-3(A) AMCD-LST Rotational Equations of Motion

ORIGINAL PAGE IS
OF POOR QUALITY

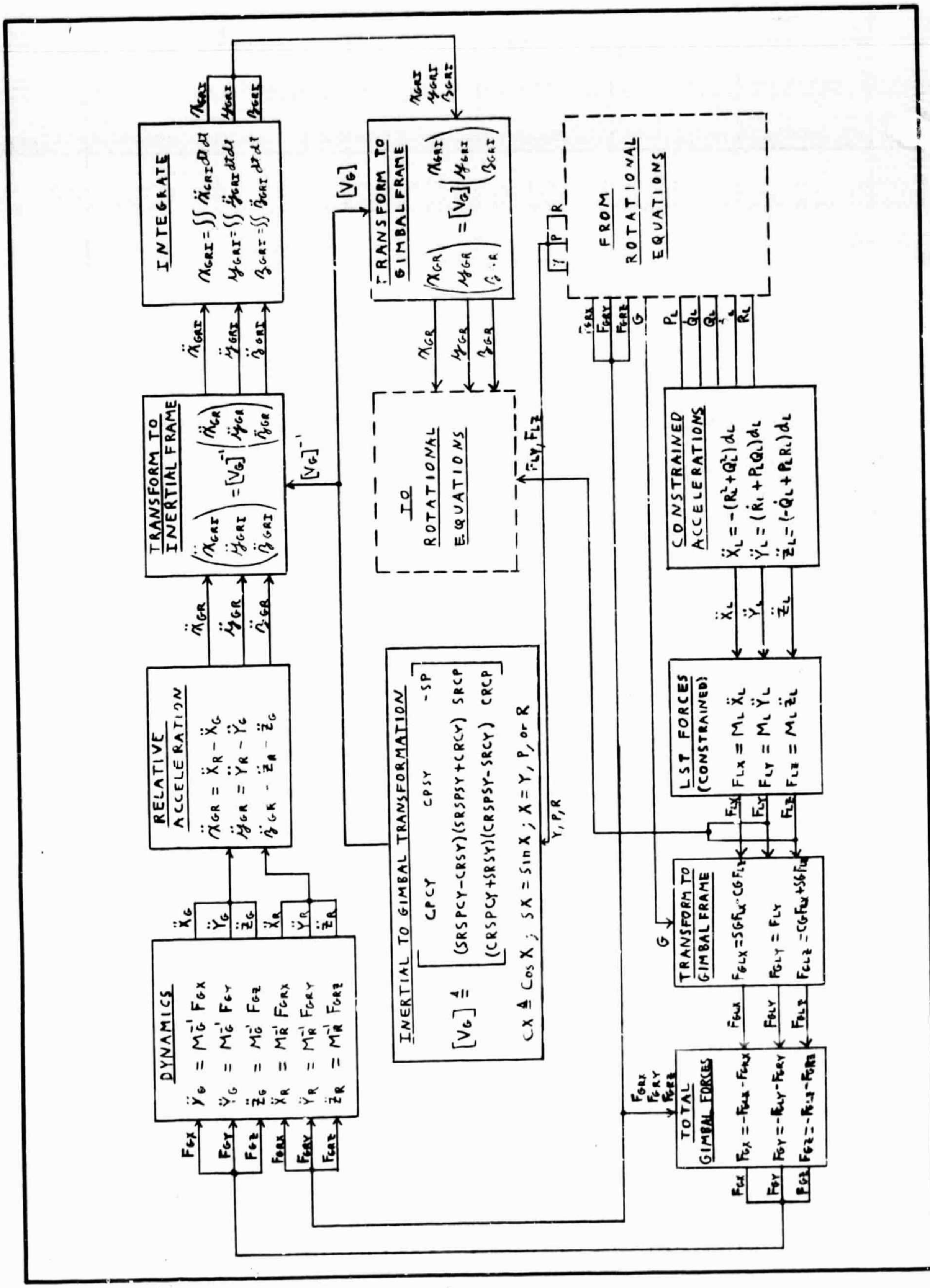

Figure 4-3(B) AMCD-LST Translational Equations of Motion

ORIGINAL PAGE IS
OF POOR QUALITY

- The arms attaching the AMCD to the LST are considered to be attached such that the resultant of forces collinear with them passes through the centers of mass of the LST and the AMCD. This assumption is tantamount to saying that the interbody coupling forces which are collinear with the arms produce no torques.

- No external forces or torques are considered to act on the system.

Kinematics

The sytem will be oriented in inertial space using four reference frames:

$X_I Y_I Z_I$: Inertial frame.

$X_G Y_G Z_G$: Frame fixed to gimbal ring with X_G normal to the gimbal plane.

$X_L Y_L Z_L$: Frame fixed to the LST with X_L out the pointing axis and Z_L toward the sun side.

$X_R Y_R Z_R$: Nonspinning frame fixed to rim spin axis such that X_R lies along the spin axis.

Orientation will be specified by orienting the gimbal ring frame with respect to inertial space then orienting everything else with respect to it.

The AMCD gimbal ring frame is oriented with respect to inertial space by using a 3-2-1 Euler order as shown in Figure 4-4. That is, the gimbal frame is first rotated about the Z_I axis through the yaw angle Y, then rotated about the Y' axis through the pitch angle P, then rotated about its X_G axis through the roll angle R. Then, the Euler angle rates are $\dot{Y}$ about Z_I, $\dot{P}$ about Y'

and $\dot{R}$ about X_G. Through $\dot{P}$ is orthogonal to both $\dot{Y}$ and $\dot{R}$, $\dot{Y}$ and $\dot{R}$ are nonorthogonal.

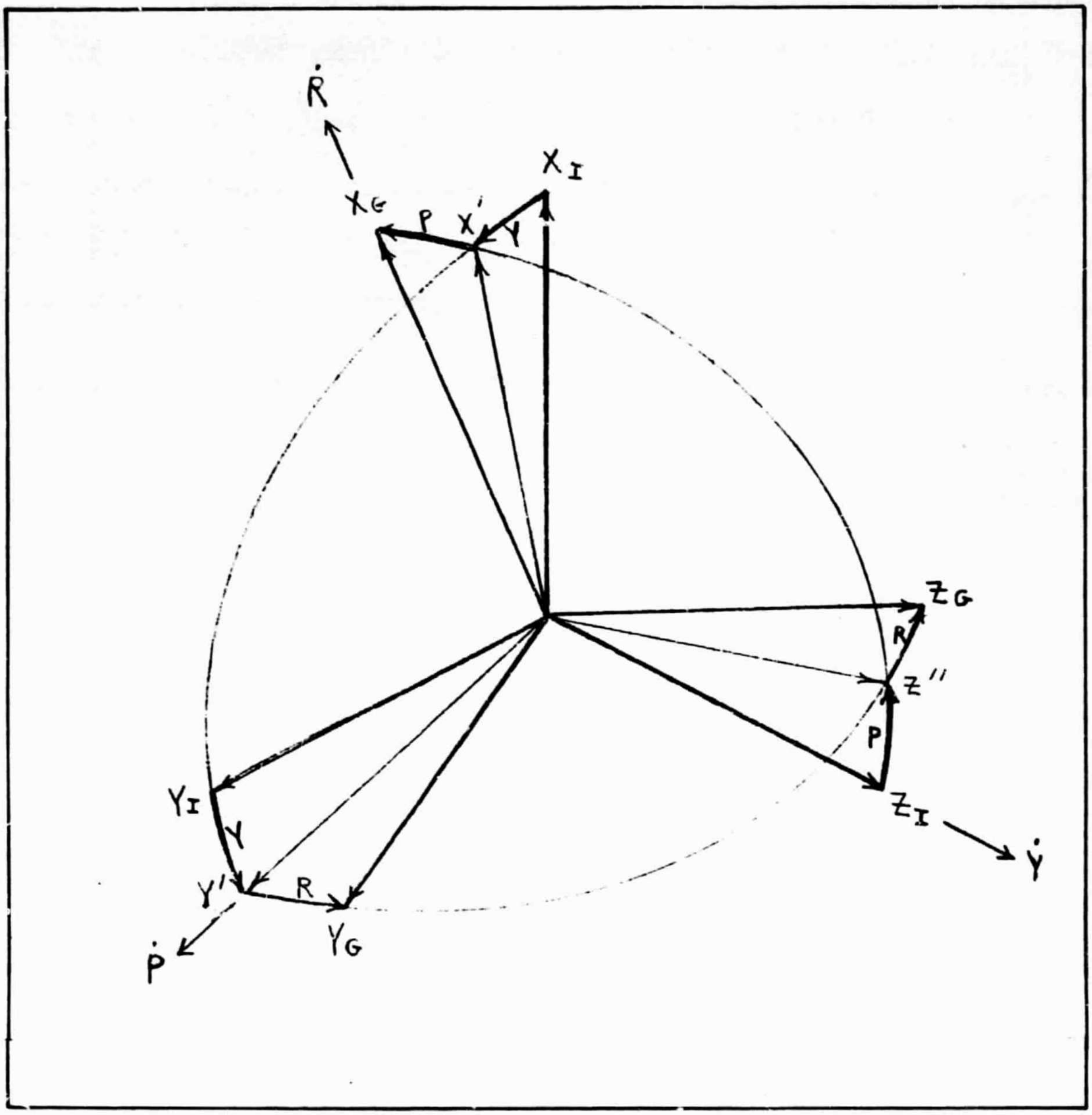

Figure 4-4 AMCD Gimbal Orientation

The transformation relating the two frames will first be developed followed by the development of the Euler angle rates in terms of the inertial body rates. This is facilitated using three

planar sketches of the rotations. The planar sketches showing the rotations, rotation rates, and transformations are shown in Figure 4-5.

From this, the transformation relating the gimbal ring frame to the inertial frame is

$$\begin{pmatrix} X_G \\ Y_G \\ Z_G \end{pmatrix} = \begin{bmatrix} 1 & 0 & 0 \\ 0 & CR & SR \\ 0 & -SR & CR \end{bmatrix} \begin{bmatrix} CP & 0 & -SP \\ 0 & 1 & 0 \\ SP & 0 & CP \end{bmatrix} \begin{bmatrix} CY & SY & 0 \\ -SY & CY & 0 \\ 0 & 0 & 1 \end{bmatrix} \begin{pmatrix} X_I \\ Y_I \\ Z_I \end{pmatrix}$$

$$= \begin{bmatrix} CP & 0 & -SP \\ SRSP & CR & SRCP \\ CRSP & -SR & CRCP \end{bmatrix} \begin{bmatrix} CY & SY & 0 \\ -SY & CY & 0 \\ 0 & 0 & 1 \end{bmatrix} \begin{pmatrix} X_I \\ Y_I \\ Z_I \end{pmatrix}$$

$$= \underbrace{\begin{bmatrix} CPCY & CPSY & -SP \\ (SRSPCY-CRSY) & (SRSPSY+CRCY) & SRCP \\ (CRSPCY+SRSY) & (CRSPSY-SRCY) & CRCP \end{bmatrix}}_{\triangleq\ [V_G].} \begin{pmatrix} X_I \\ Y_I \\ Z_I \end{pmatrix} \quad (6\text{-}1)$$

where the convention is used that $SIN(X) \triangleq SX$ and $COS(X) \triangleq CX$. From Figure 4-5, the inertial body rates of the gimbal frame are

$$(\Omega_G) \triangleq \begin{pmatrix} P_G \\ Q_G \\ R_G \end{pmatrix} = \begin{bmatrix} CP & 0 & -SP \\ SRSP & CR & SRCP \\ CRSP & -SR & CRCP \end{bmatrix} \begin{pmatrix} 0 \\ 0 \\ \dot{Y} \end{pmatrix} + \begin{bmatrix} 1 & 0 & 0 \\ 0 & CR & SR \\ 0 & -SR & CR \end{bmatrix} \begin{pmatrix} \dot{R} \\ \dot{P} \\ 0 \end{pmatrix}$$

$$= \begin{pmatrix} -SP\dot{Y}+\dot{R} \\ SRCP\dot{Y}+CR\dot{P} \\ CRCP\dot{Y}-SR\dot{P} \end{pmatrix}. \qquad (6\text{-}2)$$

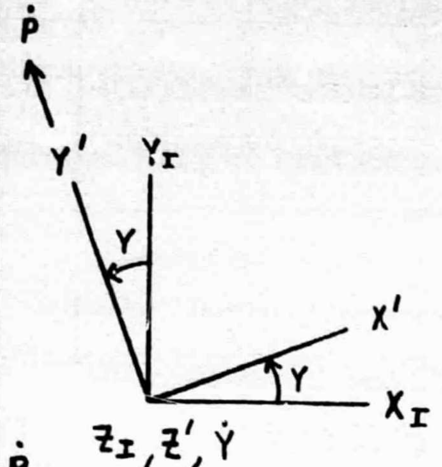

$$\begin{pmatrix} X' \\ Y' \\ Z' \end{pmatrix} = \begin{bmatrix} CY & SY & 0 \\ -SY & CY & 0 \\ 0 & 0 & 1 \end{bmatrix} \begin{pmatrix} X_I \\ Y_I \\ Z_I \end{pmatrix}$$

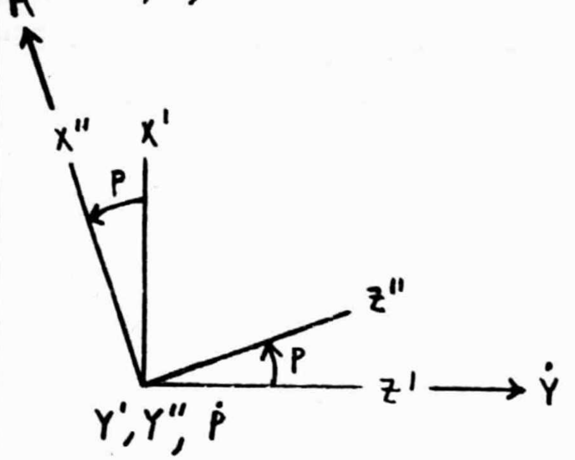

$$\begin{pmatrix} X'' \\ Y'' \\ Z'' \end{pmatrix} = \begin{bmatrix} CP & 0 & -SP \\ 0 & 1 & 0 \\ SP & 0 & CP \end{bmatrix} \begin{pmatrix} X' \\ Y' \\ Z' \end{pmatrix}$$

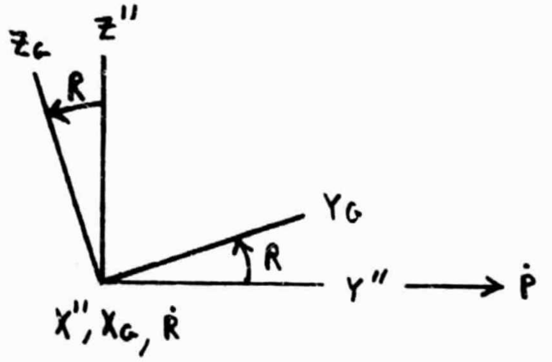

$$\begin{pmatrix} X_G \\ Y_G \\ Z_G \end{pmatrix} = \begin{bmatrix} 1 & 0 & 0 \\ 0 & CR & SR \\ 0 & -SR & CR \end{bmatrix} \begin{pmatrix} X'' \\ Y'' \\ Z'' \end{pmatrix}$$

Figure 4-5 Gimbal Planar Rotation

Now invert to get Euler rates in terms of body rates

$$
\begin{aligned}
Q_G SR &= S^2 RCP\dot{Y} + SRCR\dot{P} \\
R_G CR &= C^2 RCP\dot{Y} - CRSR\dot{P} \\
\hline
\dot{Y} &= (Q_G SR + R_G CR)/CP
\end{aligned}
\qquad (4\text{-}3)
$$

$$
\begin{aligned}
Q_G CR &= CRSRCP\dot{Y} + C^2 R\dot{P} \\
R_G SR &= SRCRCP\dot{Y} - S^2 R\dot{P} \\
\hline
\dot{P} &= (Q_G CR - R_G SR)
\end{aligned}
\qquad (4\text{-}4)
$$

$$
\dot{R} = P_G + SP\dot{Y} = P_G + \tan P(Q_G SR + R_G CR) \qquad (4\text{-}5)
$$

Arrange in matrix form

$$
(\Omega_I) \triangleq \begin{pmatrix} \dot{R} \\ \dot{P} \\ \dot{Y} \end{pmatrix} = \underbrace{\begin{bmatrix} 1 & tPSR & tPCR \\ 0 & CR & -SR \\ 0 & SR/CP & CR/CP \end{bmatrix}}_{\triangleq\ [U_I]} \begin{pmatrix} P_G \\ Q_G \\ R_G \end{pmatrix} \qquad (\ \text{-}6)
$$

The matrix $[V_G]$ of (4-1) relates the components of an arbitrary vector in the inertial frame to the components of the vector in the gimbal frame. The matrix $[U_I]$ of (4-6) relates the gimbal inertial body rates to the Euler angle rates.

The AMCD rim spin axis is oriented with respect to the gimbal ring by two <u>small</u> tilt rotations, Ψ about Z_G followed by θ about Y_R. The planar sketches showing the rotations, rotation rates, and transformations is shown in Figure 4-6.

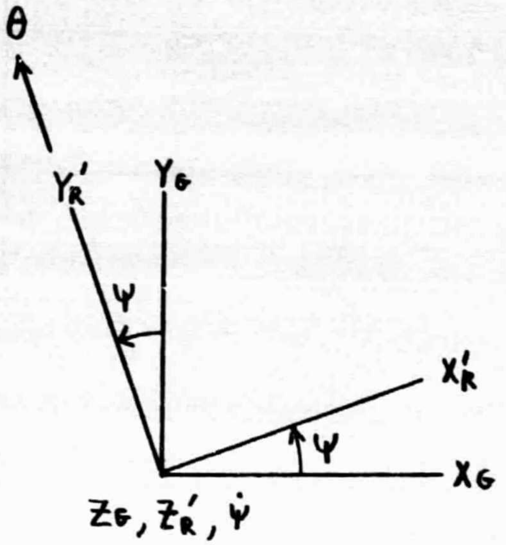

$$\begin{pmatrix} X_R' \\ Y_R' \\ Z_R' \end{pmatrix} = \begin{bmatrix} 1 & \psi & 0 \\ -\psi & 1 & 0 \\ 0 & 0 & 1 \end{bmatrix} \begin{pmatrix} X_G \\ Y_G \\ Z_G \end{pmatrix}$$

ψ is a small angle

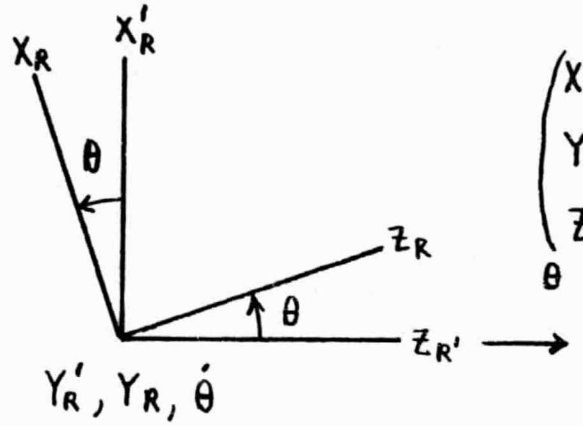

$$\begin{pmatrix} X_R \\ Y_R \\ Z_R \end{pmatrix} = \begin{bmatrix} 1 & 0 & -\theta \\ 0 & 1 & 0 \\ \theta & 0 & 1 \end{bmatrix} \begin{pmatrix} X_R' \\ Y_R' \\ Z_R' \end{pmatrix}$$

θ is a small angle

Figure 4-6 AMCD Planar Rotations

From this, the transformation relating the nonspinning rim spin axis frame to the gimbal ring frame is

$$\begin{pmatrix} X_R \\ Y_R \\ Z_R \end{pmatrix} = \begin{bmatrix} 1 & 0 & -\theta \\ 0 & 1 & 0 \\ \theta & 0 & 1 \end{bmatrix} \begin{bmatrix} 1 & \Psi & 0 \\ -\Psi & 1 & 0 \\ 0 & 0 & 1 \end{bmatrix} \begin{pmatrix} X_G \\ Y_G \\ Z_G \end{pmatrix}$$

$$= \underbrace{\begin{bmatrix} 1 & \Psi & -\theta \\ -\Psi & 1 & 0 \\ \theta & 0 & 1 \end{bmatrix}}_{\triangleq [V_A]} \begin{pmatrix} X_G \\ Y_G \\ Z_G \end{pmatrix}$$

The product $\theta\Psi$ is negligible since θ and Ψ are small. (4-7)

The inertial body rates of this frame are the inertial body rates of the gimbal ring frame plus the body rate of the rim frame with respect to the gimbal ring frame.

$$(\Omega_R) \triangleq \begin{pmatrix} P_R \\ Q_R \\ R_R \end{pmatrix} = \begin{bmatrix} 1 & \Psi & -\theta \\ -\Psi & 1 & 0 \\ \theta & 0 & 1 \end{bmatrix} \begin{pmatrix} P_G \\ Q_G \\ R_G \end{pmatrix} + \begin{bmatrix} 1 & 0 & -\theta \\ 0 & 1 & 0 \\ \theta & 0 & 1 \end{bmatrix} \begin{pmatrix} 0 \\ \dot{\theta} \\ \dot{\Psi} \end{pmatrix}$$

$$= \begin{pmatrix} P_G + \Psi Q_G - \theta R_G - \theta\dot{\Psi} \\ -\Psi P_G + Q_G + \dot{\theta} \\ \theta P_G + R_G + \dot{\Psi} \end{pmatrix} \quad (4\text{-}8)$$

Inverting,

$$\dot{\theta} = Q_R + \Psi P_G - Q_G$$

$$\dot{\Psi} = R_R - \theta P_R - R_G \quad (4\text{-}9)$$

The matrix $[V_A]$ of (4-7) relates the components of an arbitrary vector in the gimbal frame to the components of the vector in the rim frame. Equation 4-9 relates the tilt Euler angle rates to the inertial body rates of the gimbal and rim frames.

The LST frame is oriented with respect to the gimbal ring frame by a rotation through the gimbal angle β = 270°+G as shown in Figure 4-7.

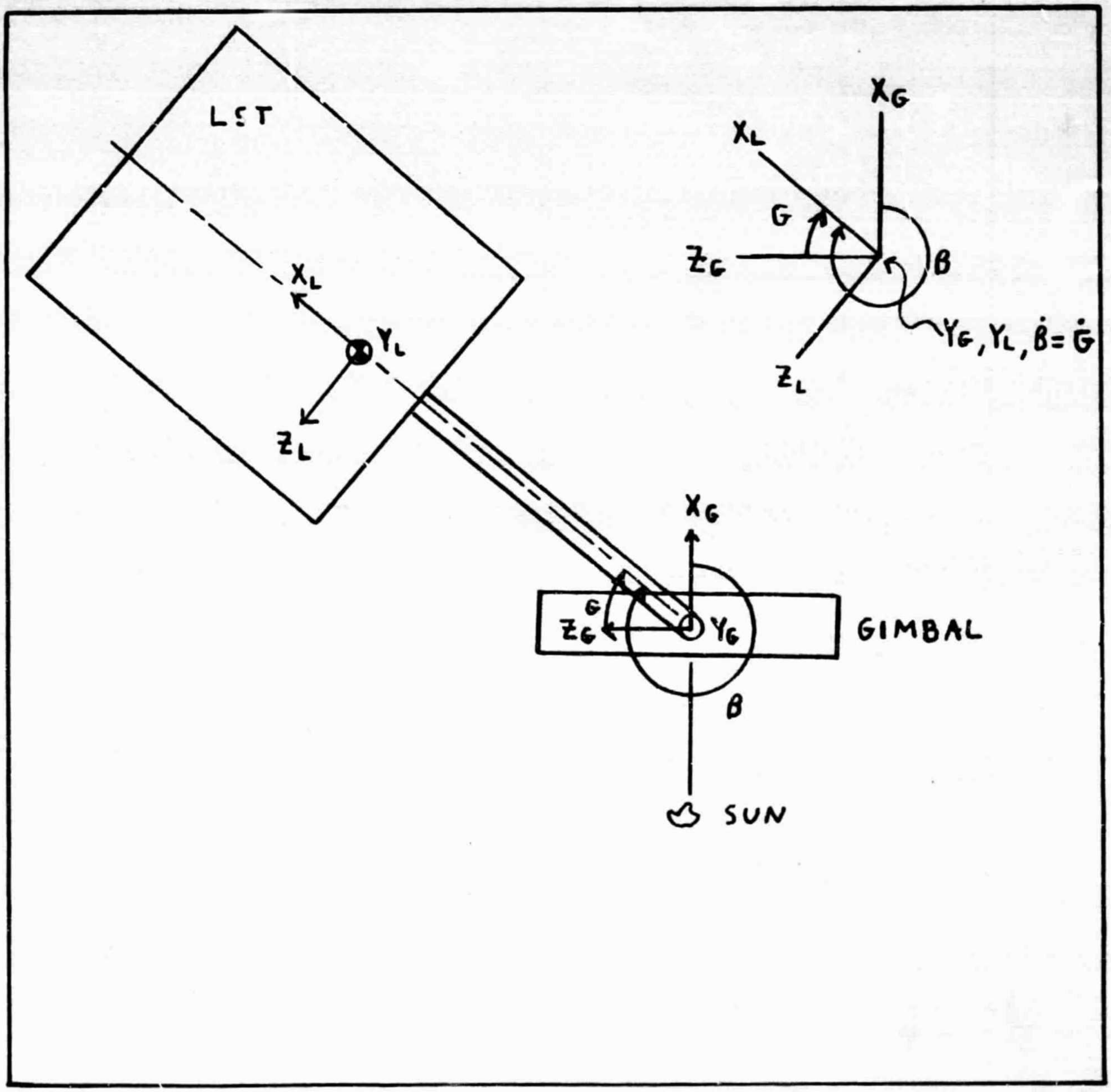

Figure 4-7 LST Orientation

From Figure 4-7,

$$\begin{pmatrix} X_L \\ Y_L \\ Z_L \end{pmatrix} = \underbrace{\begin{bmatrix} SG & 0 & CG \\ 0 & 1 & 0 \\ -CG & 0 & SG \end{bmatrix}}_{[V_L]} \begin{pmatrix} X_G \\ Y_G \\ Z_G \end{pmatrix} \tag{4-10}$$

The inertial body rates of the LST frame are the inertial body rates of the gimbal ring frame plus the body rate of the LST frame with respect to the gimbal frame

$$(\Omega_L) = \begin{pmatrix} P_L \\ Q_L \\ R_L \end{pmatrix} = \begin{bmatrix} SG & 0 & CG \\ 0 & 1 & 0 \\ -CG & 0 & SG \end{bmatrix} \begin{pmatrix} P_G \\ Q_G \\ R_G \end{pmatrix} + \begin{pmatrix} 0 \\ \dot{G} \\ 0 \end{pmatrix}$$

$$= \begin{pmatrix} SGP_G + CGR_G \\ Q_G + \dot{G} \\ -CGP_G + SGR_G \end{pmatrix} \tag{4-11}$$

Inverting,

$$\dot{G} = Q_L - Q_G \tag{4-12}$$

The matrix $[V_L]$ of (4-10) relates the components of an arbitrary vector in the gimbal ring frame to the components of the vector in the LST frame. Equation 4-12 relates the gimbal angle rate G to the inertial body rates of the LST and gimbal ring frames.

Dynamics

First, consider the equations of motion of just the suspended rim. Its free-body diagram is shown in Figure 4-8. The origin of the nonspinning AMCD rim frame is considered to be at the center of mass of the rim. The frame is oriented such that X_R lies along the spin axis, then Y_R and Z_R lie in the rim plane. The frame is not rigidly attached to the rim so that it does not spin with it; however, it does tilt with it.

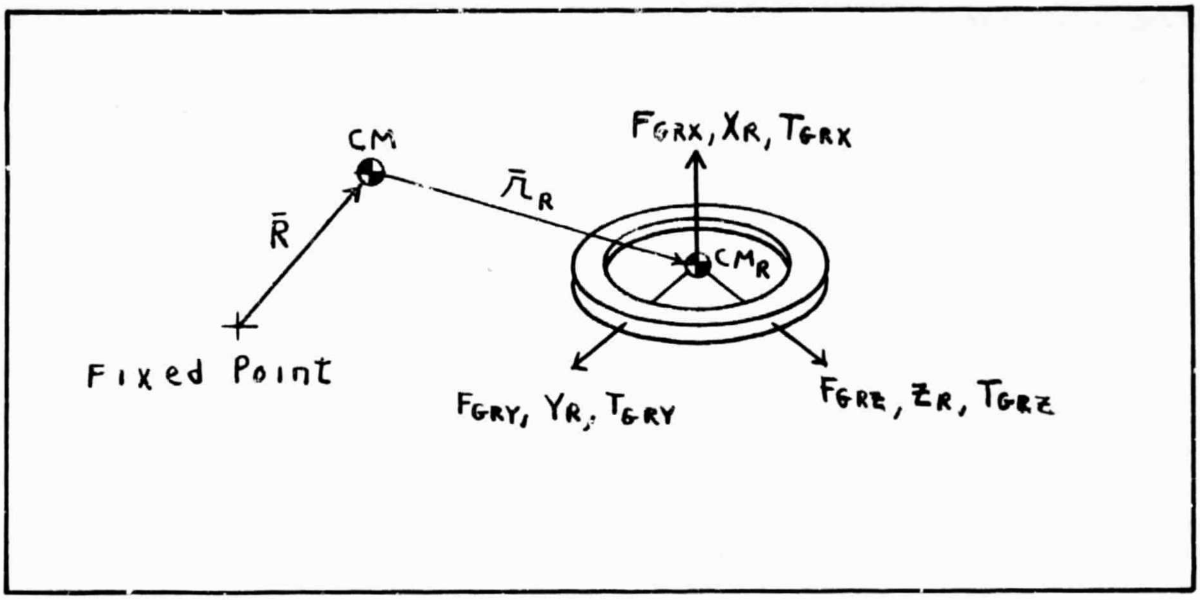

Figure 4-8 Rim Free-Body Diagram

The forces F_{GRX}, F_{GRY}, and F_{GRZ} are the control forces which the gimbal ring imparts on the rim to position it within the air gap. The torques T_{GRX}, T_{GRY}, and T_{GRZ} are the control torques which the gimbal ring imparts on the rim to spin it up and tilt it within the air gap.

The translational equations of motion are given by

$$F_{GRX} = M_R\ddot{X}_R$$

$$F_{GRY} = M_R\ddot{Y}_R$$

$$F_{GRZ} = M_R\ddot{Z}_R \tag{4-13}$$

where $\ddot{X}_R$, $\ddot{Y}_R$, and $\ddot{Z}_R$ are the components of <u>inertial</u> translational acceleration of the rim expressed in the AMCD rim frame and M_R is the mass of the rim.

The angular momentum of the rim is

$$(\overline{H}_R) = \begin{pmatrix} H_{RX} \\ H_{RY} \\ H_{RZ} \end{pmatrix} = \begin{bmatrix} I_S & & \\ & I_T & \\ & & I_T \end{bmatrix} \begin{pmatrix} P_R+P_S \\ Q_R \\ R_R \end{pmatrix} = \begin{pmatrix} I_S(P_R+P_S) \\ I_T Q_R \\ I_T R_R \end{pmatrix} \tag{4-14}$$

where I_S is the moment of inertia of the rim about the spin axis; I_T is the transverse moment of inertia of the rim; P_R, Q_R, and R_R are the components of inertial angular velocity of the $X_RY_RZ_R$ frame; and P_S is the spin rate of the rim relative to $X_RY_RZ_R$. The rotational equations of motion are given by

$$\overline{T}_{GR} = \dot{\overline{H}}_R + \overline{\Omega}_R X \overline{H}_R. \tag{4-15}$$

In matrix form, this is given by

$$(\overline{T}_{GR}) = \begin{pmatrix} T_{GRX} \\ T_{GRY} \\ T_{GRZ} \end{pmatrix} = \begin{pmatrix} I_S(\dot{P}_R+\dot{P}_S) \\ I_T\dot{Q}_R \\ I_T\dot{R}_R \end{pmatrix} + \begin{bmatrix} 0 & -R_R & Q_R \\ R_R & 0 & -P_R \\ -Q_R & P_R & 0 \end{bmatrix} \begin{pmatrix} I_S(P_R+P_S) \\ I_TQ_R \\ I_TR_R \end{pmatrix}$$

$$= \begin{pmatrix} I_S(\dot{P}_R+\dot{P}_S) \\ I_T\dot{Q}_R-(I_T-I_S)R_RP_R+I_SR_RP_S \\ I_T\dot{R}_R-(I_S-I_T)P_RQ_R-I_SP_SQ_R \end{pmatrix} \quad (4\text{-}16)$$

T_{GRX} is the torque which the gimbal ring imports about the rim spin axis to control its speed. The transverse torques T_{GRY} and T_{GRZ} are those that the gimbal ring imparts on the rim to control its tilt in the air gap.

Now consider the equations of motion of just the LST. Its free-body diagram is shown in Figure 4-9. At the gimbal point, the

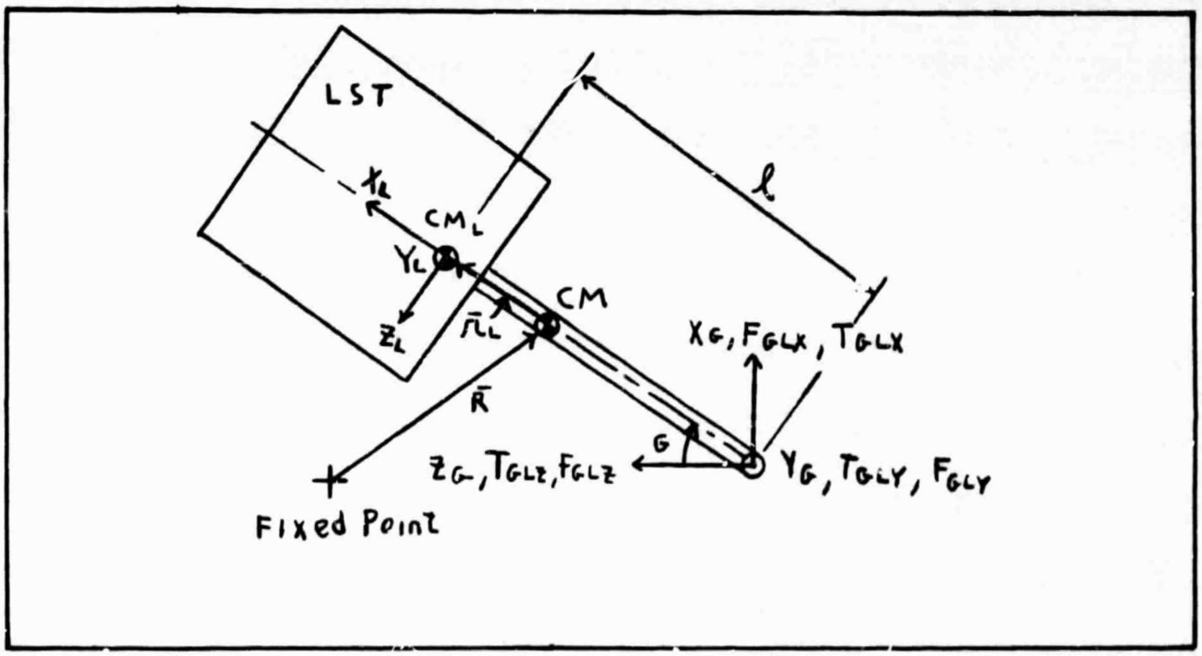

Figure 4-9 LST Free-Body Diagram

gimbal ring imparts forces F_{GLX}, F_{GLY}, F_{GLZ} and torques T_{GLX}, T_{GLY}, T_{GLZ} on the LST. The control torque T_{GLY} moves the LST with respect to the gimbal ring. The other interbody forces and torques are constraint forces and torques which hold the gimbal ring and LST together. These forces and torques are resolved into the LST fixed frame as follows (see equation 4-10):

$$\begin{pmatrix} F_{LX} \\ F_{LY} \\ F_{LZ} \end{pmatrix} = [V_L] \begin{pmatrix} F_{GLX} \\ F_{GLY} \\ F_{GLZ} \end{pmatrix} = \begin{pmatrix} F_{GLX}SG + F_{GLZ}CG \\ F_{GLY} \\ -F_{GLX}CG + F_{GLZ}SG \end{pmatrix} \tag{4-17}$$

$$\begin{pmatrix} T_{LX} \\ T_{LY} \\ T_{LZ} \end{pmatrix} = [V_L] \begin{pmatrix} T_{GLX} \\ T_{GLY} \\ T_{GLZ} \end{pmatrix} = \begin{pmatrix} T_{GLX}SG + T_{GLZ}CG \\ T_{GLY} \\ -T_{GLX}CG + T_{GLZ}SG \end{pmatrix} \tag{4-18}$$

The translational equations of motion are given by

$$F_{LX} = M_L \ddot{X}_L$$

$$F_{LY} = M_L \ddot{Y}_L$$

$$F_{LZ} = M_L \ddot{Z}_L \tag{4-19}$$

where M_L is the mass of the LST and $\ddot{X}_L$, $\ddot{Y}_L$, and $\ddot{Z}_L$ are the components of inertial translational acceleration of the LST expressed in the LST frame.

The angular momentum of the LST about its center of mass is

$$(\bar{H}_L) = \begin{bmatrix} I_{LX} & & \\ & I_{LY} & \\ & & I_{LZ} \end{bmatrix} \begin{pmatrix} P_L \\ Q_L \\ R_L \end{pmatrix} = \begin{pmatrix} I_{LX}P_L \\ I_{LY}Q_L \\ I_{LZ}R_L \end{pmatrix} \tag{4-20}$$

where I_{LX}, I_{LY}, and I_{LZ} are the moments of inertia of the LST about the X_L, Y_L, and Z_L axes and P_L, Q_L, and R_L are the components of inertial angular velocity of the $X_L Y_L Z_L$ frame.

The rotational equations of motion are given by

$$\bar{T}_L = \dot{\bar{H}}_L + \bar{\Omega}_L X \bar{H}_L \tag{4 21}$$

where $\bar{T}_L$ includes the interbody coupling torques T_{LX}, T_{LY}, T_{LZ} and the torques about the LST center of mass due to the interbody coupling forces F_{LX}, F_{LY}, and F_{LZ} which act at the gimbal point. The force F_{LX} is transmitted to the LST through two arms spaced symetrically with respect to the LST center of mass; therefore the two arms produce equal and opposite torques about Z_L which cancel. In matrix form, the rotational equations of motion are

$$(\bar{T}_L) = \begin{pmatrix} T_{LX} \\ T_{LY} \\ T_{LZ} \end{pmatrix} + \begin{pmatrix} 0 \\ \ell F_{LZ} \\ -\ell F_{LY} \end{pmatrix} = \begin{pmatrix} I_{LX}\dot{P}_L \\ I_{LY}\dot{Q}_L \\ I_{LZ}\dot{R}_L \end{pmatrix} + \begin{bmatrix} 0 & -R_L & Q_L \\ R_L & 0 & -P_L \\ -Q_L & P_L & 0 \end{bmatrix} \begin{pmatrix} I_{LX}P_L \\ I_{LY}Q_L \\ I_{LZ}R_L \end{pmatrix}$$

or

$$\begin{pmatrix} T_{LX} \\ T_{LY}+\ell F_{LZ} \\ T_{LZ}-\ell F_{LY} \end{pmatrix} = \begin{pmatrix} I_{LX}\dot{P}_L-(I_{LY}-I_{LZ})Q_LR_L \\ I_{LY}\dot{Q}_L-(I_{LZ}-I_{LX})R_LP_L \\ I_{LZ}\dot{R}_L-(I_{LX}-I_{LY})P_LQ_L \end{pmatrix} \qquad (4\text{-}22)$$

There is only one degree of freedom between the LST and the gimbal and that is about the Y_L axis. For this reason only the middle equation will be used to solve for the body rate Q_L. The other two LST body rates and accelerations are obtained by simply resolving P_G and R_G into their axes using equation (4-10) as follows:

$$\begin{aligned} P_L &= SGP_G+CGR_G \\ R_L &= -CGP_G+SGR_G \\ \dot{P}_L &= SG\dot{P}_G+CG\dot{R}_G \\ \dot{R}_L &= -CG\dot{P}_G+SG\dot{R}_G \end{aligned} \qquad (4\text{-}23)$$

Finally, consider the equations of motion of the gimbal ring. Its free-body diagram is shown in Figure 4-10. The gimbal ring frame is fixed to the gimbal ring with its origin at the gimbal

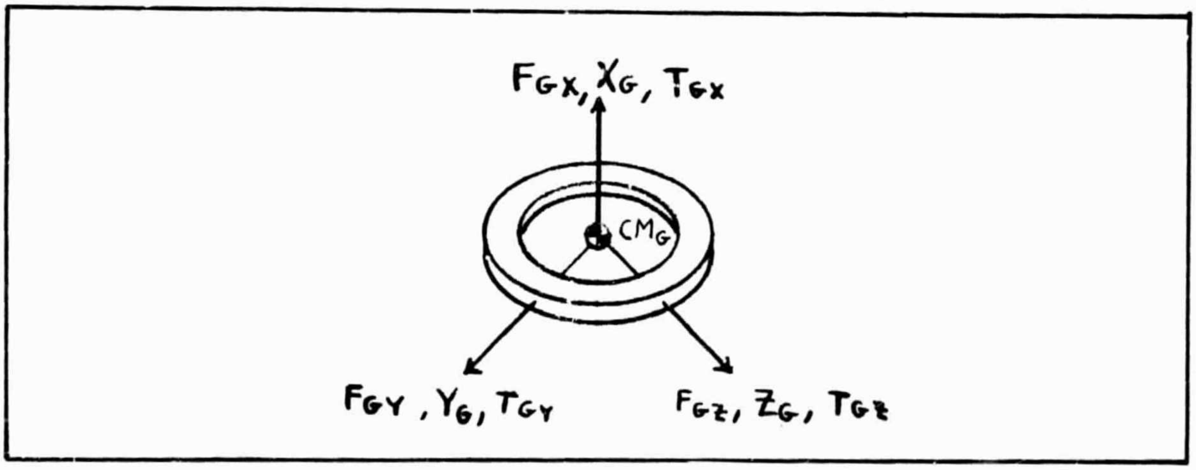

Figure 4-10 Gimbal Free-Body Diagram

ring center of mass. Y_G and Z_G are in the gimbal ring plane and X_G is normal to this plane. The forces F_{GX},F_{GY},F_{GZ} and torques T_{GX},T_{GY}, and T_{GZ} are the interbody forces and torques which the LST and rim impart on the gimbal ring and are opposite in sign to the forces and torques which the gimbal ring imparts on the LST and rim.

They are related as follows assuming small tilt angles between the gimbal ring and the rim.

$$F_{GX} = -F_{GRX} - F_{GLX}$$

$$F_{GY} = -F_{GRY} - F_{GLY}$$

$$F_{GZ} = -F_{GRZ} - F_{GLZ}$$

$$T_{GX} = -T_{GRX} - T_{GLX}$$

$$T_{GY} = -T_{GRY} - T_{GLY}$$

$$T_{GZ} = -T_{GRZ} - T_{GLZ} \qquad (4\text{-}24)$$

The translational equations of motion are

$$F_{GX} = M_G\ddot{X}_G$$

$$F_{GY} = M_G\ddot{Y}_G$$

$$F_{GZ} = M_G\ddot{Z}_G \qquad (4\text{-}25)$$

where M_G is the mass of the gimbal ring and $\ddot{X}_G$,$\ddot{Y}_G$, and $\ddot{Z}_G$ are the components of inertial translational acceleration of the gimbal ring expressed in the gimbal ring frame.

The angular momentum of the gimbal ring about its center of mass is

$$(\overline{H}_G) = \begin{bmatrix} I_{GX} & & \\ & I_{GY} & \\ & & I_{GZ} \end{bmatrix} \begin{pmatrix} P_G \\ Q_G \\ R_G \end{pmatrix} = \begin{pmatrix} I_{GX}P_G \\ I_{GY}Q_G \\ I_{GZ}R_G \end{pmatrix} \qquad (4\text{-}26)$$

where I_{GX}, I_{GY}, I_{GZ} are the moments of inertia of the gimbal ring about the X_G, Y_G, and Z_G axes and P_G, Q_G, and R_G are the components of inertial angular velocity of the $X_GY_GZ_G$ frame.

The rotational equations of motion are given by

$$\overline{T}_G = \dot{\overline{H}}_G + \overline{\Omega}_G X \overline{H}_G \qquad (4\text{-}27)$$

The interbody forces imparted by the LST on the gimbal ring either pass through the gimbal ring center of mass or form cancelling moments about the gimbal ring center of mass through the two arms. The interbody forces imparted by the rim on the gimbal ring pass through the center of mass of the gimbal ring. Thus only the interbody torques cause the gimbal ring to rotate. In matrix form, the rotational equations of motion are

$$(\overline{T}_G) = \begin{pmatrix} T_{GX} \\ T_{GY} \\ T_{GZ} \end{pmatrix} = \begin{pmatrix} I_{GX}\dot{P}_G \\ I_{GY}\dot{Q}_G \\ I_{GZ}\dot{R}_G \end{pmatrix} + \begin{bmatrix} 0 & -R_G & Q_G \\ R_G & 0 & -P_G \\ -Q_G & P_G & 0 \end{bmatrix} \begin{pmatrix} I_{GX}P_G \\ I_{GY}Q_G \\ I_{GZ}R_G \end{pmatrix}$$

$$= \begin{pmatrix} I_{GX}\dot{P}_G - (I_{GY} - I_{GZ})Q_GR_G \\ I_{GY}\dot{Q}_G - (I_{GZ} - I_{GX})R_GP_G \\ I_{GZ}\dot{R}_G - (I_{GX} - I_{GY})P_GQ_G \end{pmatrix} \qquad (4\text{-}28)$$

Assuming that all the control forces (F_{GRX},F_{GRY},F_{GRZ}) and torques (T_{GRX},T_{GRY},T_{GRZ},T_{GLY}) are known we still need the translational equation $\ddot{Y}_L$ and $\ddot{Z}_L$ to obtain a complete solvable set of rotational equations of motion. To obtain these, we assume that neither external torques nor forces are acting on the system, then the center of mass of the system is not accelerating. The inertial acceleration of the LST frame then is just the acceleration of this frame with respect to the center of mass of the system. Let its position vector with respect to the center of mass be expressed in the LST frame. Since the system center of mass is between and in line with the centers of mass of the LST and the combined center of mass of the gimbal ring and rim (see Figure 6-4), the position vector of the LST frame is always of constant length and directed out the LST X axis. It is given then by

$$\bar{r}_L = \bar{i}_L d_L \tag{4-29}$$

Its inertial velocity is given by

$$\frac{dr_L}{dt} = \dot{\bar{r}}_L + \bar{\Omega}_L X \bar{r}_L \tag{4-30}$$

and its inertial acceleration is given by

$$\frac{d^2\bar{r}_L}{dt} = \ddot{\bar{r}}_L + \dot{\bar{\Omega}}_L X \bar{r}_L + \bar{\Omega}_L X \dot{\bar{r}}_L + \bar{\Omega}_L X \dot{\bar{r}}_L + \bar{\Omega}_L X(\bar{\Omega}_L X \bar{r}_L) \tag{4-31}$$

Since the position vector has constant length $\dot{\bar{r}}_L$ and $\ddot{\bar{r}}_L$ are zero resulting in

$$\frac{d^2\bar{r}_L}{dt^2} = \dot{\bar{\Omega}}_L X \bar{r}_L + \bar{\Omega}_L X(\bar{\Omega}_L X \bar{r}_L) \tag{4-32}$$

In matrix form, this is

$$\left(\frac{d^2\bar{r}_L}{dt^2}\right) = \begin{pmatrix} \ddot{X}_L \\ \ddot{Y}_L \\ \ddot{Z}_L \end{pmatrix} = \begin{bmatrix} 0 & -\dot{R}_L & \dot{Q}_L \\ \dot{R}_L & 0 & -\dot{P}_L \\ -\dot{Q}_L & \dot{P}_L & 0 \end{bmatrix} \begin{pmatrix} d_L \\ 0 \\ 0 \end{pmatrix} + \begin{bmatrix} 0 & -R_L & Q_L \\ R_L & 0 & -P_L \\ -Q_L & P_L & 0 \end{bmatrix} \begin{bmatrix} 0 & -R_L & Q_L \\ R_L & 0 & -P_L \\ -Q_L & P_L & 0 \end{bmatrix} \begin{pmatrix} d_L \\ 0 \\ 0 \end{pmatrix}$$

$$= \begin{pmatrix} -R_L{}^2 - Q_L{}^2 \\ \dot{R}_L + P_L Q_L \\ -\dot{Q}_L + P_L R_L \end{pmatrix} d_L \qquad (4\text{-}33)$$

The control forces and torques are functions of the particular control laws used. In all cases the gimbal ring-to-LST control torque is a function of the gimbal angle (see equation 6-12).

$$G = \int \dot{G} dt = \int (Q_L - Q_G) dt \qquad (4\text{-}34)$$

Then

$$T_{GLY} = f(G, G_C) \qquad (4\text{-}35)$$

where G_C is the gimbal command.

The gimbal ring-to-rim control forces tend to position the rim in the air gap with respect to the gimbal ring. To do this, the control system needs the relative position coordinates x_{GR}, y_{GR}, and z_{GR}. Since the sensors are usually on the gimbal ring, the coordinates are expressed in the gimbal frame.

The control forces are then

$$F_{GRX} = f(x_{GR},\theta,\Psi,\theta_C,\Psi_C)$$

$$F_{GRY} = f(y_{GR})$$

$$F_{GRZ} = f(z_{GR}) \tag{4-36}$$

where θ_C and Ψ_C are rim tilt command angles.

The gimbal ring-to-rim control torques are functions of the rim spin rate and Euler angles. Then

$$T_{GRX} = f(P_S,R,R_C)$$

$$T_{GRY} = f(F_{GRX})$$

$$T_{GRZ} = f(F_{GRX}) \tag{4-37}$$

where R_C is the roll command.

Since the rim tilt angles are assumed small, the relative acceleration between the rim and the gimbal ring is given by

$$\ddot{X}_{GR} = \ddot{X}_R - \ddot{X}_G$$

$$\ddot{Y}_{GR} = \ddot{Y}_R - \ddot{Y}_G$$

$$\ddot{Z}_{GR} = \ddot{Z}_R - \ddot{Z}_G \tag{4-38}$$

where $\ddot{X}_G,\ddot{Y}_G,\ddot{Z}_G$ are found from equations 4-24 and 4-25 and $\ddot{X}_R$, $\ddot{Y}_R,\ddot{Z}_R$ are found from equations 4-13 and 4-36 . In equation 4-24 F_{GX},F_{GY}, and F_{GZ} are found from equations 4-17, 4-19, and 4-33, and 4-36.

To obtain x_{GR}, y_{GR}, and z_{GR}, we must transform $\ddot{X}_{GR}$, $\ddot{Y}_{GR}$, and $\ddot{Z}_{GR}$ into the inertial frame, integrate twice and transform the results back into the gimbal frame as follows:

Transform to inertial frame:

$$\begin{pmatrix} \ddot{X}_{GRI} \\ \ddot{Y}_{GRI} \\ \ddot{Z}_{GRI} \end{pmatrix} = [V_G]^{-1} \begin{pmatrix} \ddot{X}_{GR} \\ \ddot{Y}_{GR} \\ \ddot{Z}_{GR} \end{pmatrix} \tag{4-39}$$

Integrate twice:

$$\begin{pmatrix} x_{GRI} \\ y_{GRI} \\ z_{GRI} \end{pmatrix} = \iint \begin{pmatrix} \ddot{X}_{GRI} \\ \ddot{Y}_{GRI} \\ \ddot{Z}_{GRI} \end{pmatrix} dtdt \tag{4-40}$$

Transform back to gimbal frame:

$$\begin{pmatrix} x_{GR} \\ y_{GR} \\ z_{GR} \end{pmatrix} = [V_G] \begin{pmatrix} x_{GRI} \\ y_{GRI} \\ z_{GRI} \end{pmatrix} \tag{4-41}$$

In above $[V_G]$ is given by equation 4-1.

Expanding equations 4-39, 4-40, and 4-41, we obtain

$$\begin{pmatrix} \ddot{X}_{GRI} \\ \ddot{Y}_{GRI} \\ \ddot{Z}_{GRI} \end{pmatrix} = \begin{pmatrix} CPCY\ddot{X}_{GR} + (SRSPCY-CRSY)\ddot{Y}_{GR} + (CRSPCY+SRSY)\ddot{Z}_{GR} \\ CPSY\ddot{X}_{GR} + (SRSPSY+CRCY)\ddot{Y}_{GR} + (CRSPSY-SRCY)\ddot{Z}_{GR} \\ -SP\ddot{X}_{GR} + SRCP\ddot{Y}_{GR} + CRCP\ddot{Z}_{GR} \end{pmatrix} \tag{4-42}$$

$$\begin{pmatrix} x_{GRI} \\ y_{GRI} \\ z_{GRI} \end{pmatrix} = \begin{pmatrix} \int\int \ddot{X}_{GRI}\,dtdt \\ \int\int \ddot{Y}_{GRI}\,dtdt \\ \int\int \ddot{Z}_{GRI}\,dtdt \end{pmatrix} \tag{4-43}$$

$$\begin{pmatrix} x_{GR} \\ y_{GR} \\ z_{GR} \end{pmatrix} = \begin{pmatrix} CPCYx_{GRI} + CPSYy_{GRI} - SPz_{GRI} \\ (SRSPCY-CRSY)x_{GRI} + (SRSPSY+CRCY)y_{GRI} + SRCPz_{GRI} \\ (CRSPCY+SRSY)x_{GRI} + (CRSPSY-SRCY)y_{GRI} + CRCPz_{GRI} \end{pmatrix} \tag{4-44}$$

Finally, to obtain the relative spin rate between the rim and the rim frame we must subtract P_R, the inertial angular velocity of the rim frame, from P_R+P_S, the inertial angular velocity of the rim. From equation 4-8, a kinematical constraint equation, we obtain

$$P_R = P_G + \Psi Q_G - \theta R_G - \theta\dot{\Psi} \tag{4-45}$$

Then, the relative spin rate between the rim frame and the rim is

$$P_S = \int (\dot{P}_R + \dot{P}_S)\,dt - P_R \tag{4-46}$$

This completes the derivation of the equations of motion. The equations are collected as a set in the summary section at the beginning of this section. There, they are also classified and grouped in a manner to indicate the solution flow.